AIAA JOURNAL
Vol. 49, No. 4, April 2011

Introducing Loading Uncertainty in Topology Optimization

Peter D. Dunning,* H. Alicia Kim,† and Glen Mullineux‡
University of Bath, Bath, England BA2 7AY, United Kingdom

DOI: 10.2514/1.J050670

Uncertainty is an important consideration in structural design and optimization to produce robust and reliable solutions. This paper introduces an efficient and accurate approach to robust structural topology optimization. The objective is to minimize expected compliance with uncertainty in loading magnitude and applied direction, where uncertainties are assumed normally distributed and statistically independent. This new approach is analogous to a multiple load case problem where load cases and weights are derived analytically to accurately and efficiently compute expected compliance and sensitivities. Illustrative examples using a level-set-based topology optimization method are then used to demonstrate the proposed approach.

Nomenclature

A	=	material property tensor
a	=	element volume
$E[x]$	=	expected value of x
f	=	surface tractions
$\{f\}$	=	loading vector
f_i	=	entry in loading vector
H	=	Heaviside function
J	=	structural compliance
$[K]$	=	stiffness matrix
m	=	stiffness matrix order
n	=	number of loads with uncertainty
$P(x)$	=	probability density function of x
p	=	body forces
u	=	displacement field
$\{u\}$	=	displacement vector
V	=	velocity function
Vol^*	=	material volume limit
v	=	virtual displacement field
w	=	weighting factor
β	=	shape parameter
Γ	=	structural boundary
Δt	=	time step
ε	=	strain tensor
ζ	=	positive value
θ	=	angle of load application
θ_x, θ_y	=	horizontal and vertical directions
$\kappa_{i,j}$	=	entry in the inverse stiffness matrix
λ	=	constant to enforce volume constraint
μ	=	mean loading magnitude
μ_θ	=	mean loading direction
σ	=	standard deviation of loading magnitude
σ_θ	=	standard deviation of loading direction
ϕ	=	implicit function
Ω, Ω_s	=	structural domain

I. Introduction

THE world is full of uncertainties and structures need to be designed and optimized to be robust and reliable when operating in an uncertain environment. The traditional engineering approach to account for uncertainties is to employ a factor of safety. While this philosophy has produced many successful structures, the modern era demands more efficient designs that minimize waste in order to meet pressures from both economic and environmental factors. In this context the safety factor approach may be inadequate and there is increasing interest in an alternative probabilistic approach that includes a clearer understanding of uncertainties during design and optimization.

Various probabilistic approaches have been developed to account for different types of uncertainty in structural design and optimization methods [1], however, the paradigm had not been applied to structural topology optimization methods until recently. Topology optimization is becoming a popular design tool as its flexibility provides the greatest opportunity to maximize performance. This is particularly relevant to the design of aerospace components, as structural performance and weight is of critical importance. Practical structural topology optimization problems are usually solved via computational means and various methods have been developed for truss and continuum type structures and used to solve a wide range of problems [2–4], including wing box rib design [5] and wing box reinforcement for enhanced roll maneuvers [6]. It is not the purpose of this introduction to review the history of topology optimization development and its various applications. However, the interested reader is directed to [2], which contains an extensive bibliography on the subject.

At present there are two main approaches that consider uncertainties in structural topology optimization. The first is to introduce a number of reliability constraints based on probability of failure, often referred to as reliability-based topology optimization (RBTO) [7]. These methods often aim to minimize the weight or volume of a structure, while ensuring the probability of failure is less than a prescribed value. The failure probability constraint is a function of the uncertain parameters and is usually recast to ensure the reliability of the structure is greater than a required value. Various failure modes have been considered in RBTO methods, including critical limits on deformation [8,9], natural frequency [9,10] and stiffness [10,11]. Although reliability constraints can be difficult to handle during an optimization process, several techniques have been developed to improve the efficiency and robustness of RBTO. A popular technique is to approximate the reliability using the first-order reliability method (FORM) [7], which is itself an optimization problem and can be efficiently included in RBTO methods using the performance measure approach [8,9]. The main advantage of FORM is that analytical sensitivities of the reliability constraint are often available, leading to significant efficiency benefits. However, FORM only considers the mean and variance of uncertain parameters and is not appropriate when higher statistical moments have a significant effect on the failure mode or exact probability data is unavailable. When exact data is unavailable a nonprobabilistic approach can be adopted, where probability functions are assumed convex and bounded [12]. This method has also been combined with the proba-

Presented as Paper 2010-2843 at the 6th AIAA Multidisciplinary Design Optimization Specialist Conference, Orlando, FL, 12–15 April 2010; received 3 June 2010; revision received 16 November 2010; accepted for publication 9 December 2010.

*Ph.D. Student, Department of Mechanical Engineering. Member AIAA.
†Lecturer, Department of Mechanical Engineering. Senior Member AIAA.
‡Professor, Department of Mechanical Engineering.

bilistic approach, providing a more general method for reliability-based optimization [13]. The RBTO method has also recently been extended to include a system reliability constraint, which is composed of a number of component reliability constraints connected in series [14].

RBTO methods have been successfully applied to efficiently solve various structural optimization problems in the presence of uncertain parameters. However, RBTO relies on defining one or more failure states that are functions of the uncertain parameters and it is sometimes difficult to immediately define a meaningful failure state. When a failure state is not defined, an alternative approach to RBTO is to consider a probabilistic objective that is a function of the uncertain parameters. This approach is often referred to as robust optimization. Popular choices for robust objective functions are to minimize the expected or maximum performance and both approaches have been used when solving the classic minimization of compliance problem with uncertain variables [15,16].

Various parameters can affect the robustness and reliability of a structure, including loading, geometry and material properties [1]. Loading uncertainties are most widely studied, although the level of uncertainty is often limited to loading magnitude. However, uncertainty in loading direction can be simulated by considering orthogonal uncertain loads with zero mean [10]. This approach may be appropriate for some problems, however, the orthogonal loads are often uncorrelated and the relevance to the directional uncertainty of a single load can be unclear. For nonprobabilistic uncertainties, loading direction has been considered using the multi-ellipsoid convex model [17], which does allow for some interaction between orthogonal loads.

For the robust optimization approach, methods for approximating probabilistic directional uncertainties include using a discrete probability function [18], discretization of a continuous probability function using a sampling method [15,19] and an approximation by a quadrature technique [20]. These discretized approaches transform the optimization problem into a multiple load case one, which can be solved for the minimization of expected performance problem [15,18]. To achieve a level of accuracy when discretizing continuous probability functions, increasing the number of sampling points or a higher-order quadrature rule is required. This consequently increases the number of load cases that must be considered. Thus, in the presence of a large number of uncertain loads the computational cost associated with the discretization approach can quickly become prohibitive [15,19].

The motivation of this paper is to create an efficient method for considering loading magnitude and directional uncertainty in topology optimization in order to produce robust solutions. The classic minimization of compliance problem is considered with uncertainties being introduced into the objective function and described by continuous normal probability functions. The proposed method alleviates the computational burden of discretization techniques when there are a large number of uncertain loads and a high degree of accuracy is required.

II. Topology Optimization with Uncertainty in Loading

A. Robust Optimization Problem

First we state the deterministic problem without including uncertainties. The problem considered is to minimize compliance or total strain energy, subject to a constraint on the available material, or structural volume. This problem has been widely studied in the literature [2–4]:

$$\begin{gathered}\text{minimize: } J(u) = \int_\Omega A\varepsilon(u)\varepsilon(u)\,\mathrm{d}\Omega \\ \text{s.t.: } \int_\Omega \mathrm{d}\Omega \le \mathrm{Vol}^* \\ \int_\Omega A\varepsilon(u)\varepsilon(v)\,\mathrm{d}\Omega = \int_\Omega pv\,\mathrm{d}\Omega + \int_\Gamma fv\,\mathrm{d}\Gamma \end{gathered} \tag{1}$$

Where Ω is the structure domain, Γ the structure boundary, A the material property tensor, $\varepsilon(u)$ the strain tensor, u the displacement field that is a unique solution to the linear elastic system, v is any kinematically admissible displacement field, p the body forces, f the surface tractions and Vol^* the limit on material volume.

The aim of this work is to introduce uncertainties in loading magnitude and direction in the deterministic compliance problem, Eq. (1). One common approach of treating uncertainties for the compliance problem is to minimize expected performance [15,18,20–25]. This produces a robust structure that has good average performance, thus robust against the uncertainties. Therefore we formulate the objective function to be expected compliance, Eq. (2). Here we assume the equilibrium constraint is satisfied for all possible solutions and there are no body forces:

$$\begin{gathered}\text{minimize: } E[J(u,f)] = \int_f J(u,f)P(f)\,\mathrm{d}f \\ \text{s.t.: } \int_\Omega \mathrm{d}\Omega \le \mathrm{Vol}^* \end{gathered} \tag{2}$$

$$\int_\Omega A\varepsilon(u)\varepsilon(v)\,\mathrm{d}\Omega = \int_\Gamma fv\,\mathrm{d}\Gamma \tag{3}$$

where $E(x)$ is the expected value of uncertain variable x and $P(x)$ is the probability density function (pdf) of x.

A traditional stochastic approach to solve this problem with continuous pdfs is to discretize the continuous distribution [15,18,19]. The robust problem then naturally transforms into a multiple load case problem, where each load case is a discrete realization of the pdf. This approach is often referred to as stochastic programming or optimization [15,18,19]. However, it is not straight forward to select the load cases to ensure all critical cases are considered to obtain an accurate approximation of the original continuous problem.

We introduce an analytical approach that accounts for continuous pdfs. This approach avoids approximation or simplification of the original problem and hence, ensures that all critical load cases are considered. We assume that the uncertainties are represented by normal distributions.

To perform the analytical approach we assume the linear elastic system, Eq. (3) is solved by the finite element method:

$$\{f\} = [K]\{u\} \tag{4}$$

where $\{f\}$ is the loading vector, $\{u\}$ the displacement vector and $[K]$ is a symmetric stiffness matrix with order m, which is the number of degrees of freedom. A discretized expression for compliance can be written in terms of $\{f\}$ and $[K]$ using Eq. (4):

$$J(u,f) = \{f\}^T[K]^{-1}\{f\} = \sum_{i=1}^{m}\sum_{j=1}^{m}\kappa_{i,j}f_if_j \tag{5}$$

where $\kappa_{i,j}$ is an entry of the inverse stiffness matrix and i and j are row and column numbers, respectively.

B. Uncertainty in Magnitude of Loading

We first derive a formulation for expected compliance under statistically independent uncertainties in magnitude of loading, which are described by Gaussian normal distributions with mean μ_i and standard deviation σ_i. Expected compliance including uncertainty in magnitude of loading is stated using the discrete form for compliance of Eq. (5):

$$E[J(u,f)] = \int_{f_n}\cdots\int_{f_1}\sum_{i=1}^{m}\sum_{j=1}^{m}\kappa_{i,j}f_if_j\prod_{i=1}^{n}P(f_i)\,\mathrm{d}f_1\ldots\mathrm{d}f_n \tag{6}$$

where f_i are loads that can have uncertain magnitude. Using integration by parts three times for the first uncertain load f_1, Eq. (6) becomes

$$E[J(u,f)] = \int_{f_2} \dots \int_{f_n} \left[\left(f_1^2 \kappa_{1,1} + 2 f_1 \sum_{i=2}^{m} \kappa_{1,i} f_i + \sum_{i=2}^{m} \sum_{j=2}^{m} \kappa_{i,j} f_i f_j \right) \int P(f_1)\, \mathrm{d}f_1 - 2 \left(f_1 \kappa_{1,1} + \sum_{i=2}^{m} \kappa_{1,i} f_i \right) \iint P(f_1)\, \mathrm{d}f_1 + 2\kappa_{1,1} \iiint P(f_1)\, \mathrm{d}f_1 \right] \prod_{i=2}^{n} P(f_i)\, \mathrm{d}f_2 \dots \mathrm{d}f_n \tag{7}$$

Evaluating Eq. (7) between limits $\mu_1 \pm \zeta$ and letting ζ go to infinity yields

$$E[J(u,f)] = \int_{f_2} \dots \int_{f_n} \left[(\mu_1^2 + \sigma_1^2)\kappa_{1,1} + 2\mu_1 \sum_{i=2}^{m} \kappa_{1,i} f_i + \sum_{i=2}^{m} \sum_{j=2}^{m} \kappa_{i,j} f_i f_j \right] \prod_{i=2}^{n} P(f_i)\, \mathrm{d}f_2 \dots \mathrm{d}f_n \tag{8}$$

Repeating the integration process for each load with uncertain magnitude, expected compliance simplifies to the following expression:

$$E[J(u,f)] = \sum_{i=1}^{m} \sum_{j=1}^{m} \kappa_{i,j} \mu_i \mu_j + \sum_{i=1}^{m} \kappa_{i,i} \sigma_i^2 \tag{9}$$

Equation (9) reveals that expected compliance can be evaluated by summing values from $n+1$ deterministic load cases, where n is the number of loads with nonzero variance ($\sigma_i \neq 0$). The first load case is the simultaneous application of mean loads and the subsequent n cases correspond to a single load equal to σ_i applied at the location of uncertain load i. Therefore, the robust optimization problem of Eq. (2) is transformed into a multiple load case problem that can be solved by most existing topology optimization methods:

$$\begin{aligned} &\text{minimize}: E[J(u,f)] = J(u,\mu) + \sum_{i=1}^{n} J(u_i, \sigma_i) \\ &\text{s.t.:} \int_{\Omega} \mathrm{d}\Omega \leq \mathrm{Vol}^* \end{aligned} \tag{10}$$

where $J(u,\mu)$ is the compliance computed from mean loading conditions and $J(u_i, \sigma_i)$ is the compliance for a single load of magnitude σ_i. This result is not surprising, as it is similar to those found in the literature for truss structures under loading magnitude uncertainty, where the first two moments of uncertain loads are considered [15,24]. This formulation offers an efficient method for evaluating expected compliance using the minimum number of deterministic load cases where loads have uncertain magnitude described by a normal distribution.

C. Uncertainty in Direction of Loading

This section derives an efficient approach for calculating expected compliance in the presence of uncertainty in direction of loading. First we define directional uncertainty of a load in two-dimensional space in terms of its angle of application θ, where $\theta = 0$ refers to the positive horizontal direction. Expected compliance of a structure under n loads with directional uncertainty can be written as

$$E[J(u,f,\theta)] = \int_{\theta_n} \dots \int_{\theta_1} J(u,f,\theta) \prod_{i=1}^{n} P(\theta_i)\, \mathrm{d}\theta_1 \dots \mathrm{d}\theta_n \tag{11}$$

where $P(\theta)$ is a pdf for directional uncertainty. Here we assume that $P(\theta_i)$ is a Gaussian normal distribution with mean direction $\mu_{\theta,i}$ and standard deviation $\sigma_{\theta,i}$ and all uncertain variables, θ_i are statistically independent. A single load with magnitude f, but applied in an arbitrary direction can be written in terms of two orthogonal loads. For simplicity we assume one load is defined in the horizontal x direction and the other in the vertical y direction:

$$f_x(f,\theta) = f\cos(\theta) \qquad f_y(f,\theta) = f\sin(\theta) \tag{12}$$

We construct the load vector $\{f\}$ such that odd entries of the vector correspond to horizontal loads and even entries to vertical loads. As we are only interested in linear elastic structures, the stiffness matrix $[K]$ and its inverse are symmetrical. Substituting the orthogonal loads, Eq. (12), into the discrete form of compliance, Eq. (5), results in

$$J(u,f,\theta) = \sum_{i=1}^{m/2} \sum_{j=1}^{m/2} f_i f_j (\kappa_{ix,jx}\cos(\theta_i)\cos(\theta_j) + \kappa_{iy,jy}\sin(\theta_i)\sin(\theta_j) + 2\kappa_{ix,jy}\cos(\theta_i)\sin(\theta_j)) \tag{13}$$

where $ix = 2i-1$ and $iy = 2i$.

Substituting Eq. (13) into Eq. (11), the integral for expected compliance can be evaluated by substituting the complex exponential forms of the trigonometric functions. We take the integration limits of each uncertain variable to be $\theta_i = \mu_{\theta,i} \pm \pi$, which integrates over the full revolution of 2π. The result of the integral for expected compliance, Eq. (11) involves error functions in the form: $\mathrm{erf}(\pi/\sqrt{2}\sigma_{\theta,i})$. However, if at least 3 standard deviations either side of the mean direction are contained within the full revolution, $3\sigma_{\theta,i} \leq \pi$, then the error function evaluates to at least 0.9973, which can be approximated as one. The integral then simplifies to

$$\begin{aligned} E[J(u,f,\theta)] = 1/2 \sum_{i=1}^{m/2} f_i^2 [&\kappa_{ix,ix}(1 + \exp(-2\sigma_{\theta i}^2)\cos(2\mu_{\theta i})) \\ &+ \kappa_{iy,iy}(1 - \exp(-2\sigma_{\theta i}^2)\cos(2\mu_{\theta i})) \\ &+ 2\kappa_{ix,iy}(\exp(-2\sigma_{\theta i}^2)\sin(2\mu_{\theta i}))] \\ &+ \sum_{i=1}^{m/2} \sum_{j=1, j\neq i}^{m/2} (f_i f_j \exp(-\sigma_{\theta i}^2/2)\exp(-\sigma_{\theta j}^2/2)) \\ &\times [\kappa_{ix,jx}(\cos(\mu_{\theta i})\cos(\mu_{\theta j})) + \kappa_{iy,jy}\sin(\mu_{\theta i})\sin(\mu_{\theta j}) \\ &+ 2\kappa_{ix,jy}\cos(\mu_{\theta i})\sin(\mu_{\theta j})] \end{aligned} \tag{14}$$

We now proceed to define a number of load cases whose compliance values sum to the expected value derived in Eq. (14). This is achieved by subtracting the compliance values for each load case from the expected compliance. We define the first load case as the deterministic one where each entry in the load vector is multiplied by an exponential function of the variance:

$$J_1(u,\bar{f},\mu_\theta) = \{\bar{f}\}^T [K]^{-1} \{\bar{f}\} \quad \bar{f}_i = f_i \exp(-\sigma_{\theta i}^2/2) \tag{15}$$

The compliance computed for this load case using Eq. (13) is

$$\begin{aligned} J_1(u,\bar{f},\mu_\theta) = \sum_{i=1}^{m/2} \sum_{j=1}^{m/2} &(f_i f_j \exp(-\sigma_{\theta i}^2/2)\exp(-\sigma_{\theta j}^2/2)) \\ &\times [\kappa_{ix,jx}(\cos(\mu_{\theta i})\cos(\mu_{\theta j})) + \kappa_{iy,jy}\sin(\mu_{\theta i})\sin(\mu_{\theta j}) \\ &+ 2\kappa_{ix,jy}\cos(\mu_{\theta i})\sin(\mu_{\theta j})] \end{aligned} \tag{16}$$

The compliance from the first load case, Eq. (16), is now subtracted from the expected compliance, Eq. (14), leaving the compliance value to be computed by the remaining load cases. After some manipulation the subtraction equates to

$$E[J(u,f,\theta)] - J_1(u,\bar{f},\mu_\theta) = \sum_{i=1}^{m/2} [\kappa_{ix,ix}(w_{1,i}\cos^2(\mu_{\theta i}) + w_{2,i}) + \kappa_{iy,iy}(w_{1,i}\sin^2(\mu_{\theta i}) + w_{2,i}) + 2\kappa_{ix,iy}(w_{1,i}\sin(\mu_{\theta i})\cos(\mu_{\theta i}))] \tag{17}$$

where the values of w are defined as

$$w_{1,i} = f_i^2(\exp(-2\sigma_{\theta i}^2) - \exp(-\sigma_{\theta i}^2)) \tag{18}$$

$$w_{2,i} = f_i^2(1 - \exp(-2\sigma_{\theta i}^2))/2 \tag{19}$$

We now define a second set of n load cases by applying a load of unit magnitude at the deterministic location and in the mean direction of each uncertain load in turn. The compliance value computed for each of these load cases, using Eq. (13), is multiplied by $w_{1,i}$ producing

$$J_{2,i}(u, 1, \mu_{\theta,i}) = \kappa_{ix,ix}(w_{1,i}\cos^2(\mu_{\theta i})) + \kappa_{iy,iy}(w_{1,i}\sin^2(\mu_{\theta i})) + 2\kappa_{ix,iy}(w_{1,i}\sin(\mu_{\theta i})\cos(\mu_{\theta i})) \tag{20}$$

Subtracting the sum of compliance values calculated by Eq. (20) for all loads with uncertain applied direction from Eq. (17) results in

$$E[J(u, f, \theta)] - J_1(u, \bar{f}, \mu_\theta) - \sum_{i=1}^{n} J_{2,i}(u, 1, \mu_{\theta,i}) = \sum_{i=1}^{m/2} w_{2,i}[\kappa_{ix,ix} + \kappa_{iy,iy}] \tag{21}$$

Finally, two further sets of load cases are required to complete the computation of expected compliance. These load cases are defined by applying a load of unit magnitude at the location of each uncertain load in the horizontal ($\theta_x = 0,\ \pi$) and vertical ($\theta_y = \pi/2,\ 3\pi/2$) directions separately. The compliance values for these two load cases are computed for each uncertain load using Eq. (13), and multiplied by $w_{2,i}$ producing

$$J_{x,i}(u, 1, \theta_x) = w_{2,i}\kappa_{ix,ix} \qquad J_{y,i}(u, 1, \theta_y) = w_{2,i}\kappa_{iy,iy} \tag{22}$$

This completes the computation of expected compliance considering uncertainty in loading direction, Eq. (14), using a series of separate load cases. In the general case a maximum of $1 + 3n$ load cases is required where n is the number of loads with uncertain direction. The first load case is the application of deterministic loads multiplied by exponential functions of the variance, Eq. (15), and each subsequent set of three load cases are applied at the location of the uncertain load. The subsequent loads have a magnitude of one and are applied in the mean, horizontal and vertical directions in turn. Using Eqs. (16), (20), and (22) the expected compliance becomes a weighted sum of the $1 + 3n$ load cases:

$$E[J(u, f, \theta)] = J_1(u, \bar{f}, \theta) + \sum_{i=i}^{n}[w_{1,i}J_{2,i}(u, 1, \mu_{\theta i}) + w_{2,i}(J_{x,i}(u, 1, \theta_x) + J_{y,i}(u, 1, \theta_y))] \tag{23}$$

The number of load cases can be reduced by one for every value of $\mu_{\theta i}$ that is equal to θ_x or θ_y by simply combining load cases and weights appropriately. Also if all values of $\sigma_{\theta,i}$ are zero, then Eq. (23) reduces to a single load case equal to the compliance of the deterministic case, Eq. (5).

D. Combined Uncertainty in Loading

We now use the result of Eq. (9) to include magnitude uncertainty in the formulation for expected compliance under directional uncertainty. Starting with Eq. (23) the inclusion of loading magnitude uncertainties yields

$$E[J(u, f, \theta)] = \int_{f_n} \cdots \int_{f_1} E[J(u, f, \theta)] \prod_{i=1}^{n} P(f_i)\, \mathrm{d}f_1 \ldots \mathrm{d}f_n \tag{24}$$

Equation (24) is evaluated using the results of Eqs. (9) and (23) for each uncertain magnitude between limits $\mu_1 \pm \zeta$ and letting ζ go to infinity results in an equation with the same format as Eq. (23) with the following modified weights that account for the uncertainty in loading magnitude:

$$\begin{aligned} \bar{f}_i &= \mu_i \exp(-\sigma_{\theta i}^2/2) \\ w_{1,i} &= \mu_i^2(\exp(-2\sigma_{\theta i}^2) - \exp(-\sigma_{\theta i}^2)) + \sigma_i^2 \exp(-2\sigma_{\theta i}^2) \\ w_{2,i} &= 1/2(\mu_i^2 + \sigma_i^2)(1 - \exp(-2\sigma_{\theta i}^2)) \end{aligned} \tag{25}$$

It is apparent that the uncertainties in magnitude do not increase the number of load cases required to compute expected compliance when directional uncertainties are already included. Also, if all values of σ_i are zero then the expected compliance in the presence of directional uncertainties only is recovered, Eq. (23). Correspondingly, if all values of $\sigma_{\theta i}$ are zero, then the expected compliance in the presence of exclusively loading magnitude uncertainties, Eq. (9), is also recovered. Therefore, Eq. (23) with weights defined by Eqs. (25) computes an accurate value for the expected compliance using a maximum of $1 + 3n$ load cases, where n loads can have uncertainties in both magnitude and direction. This expression for expected compliance is used to transform the robust optimization problem, Eq. (2), into an equivalent multiple load case one:

$$\text{minimize: } E[J(u, f, \theta)] = J_1(u, \bar{f}, \theta) + \sum_{i=i}^{n}[w_{1,i}J_{2,i}(u, 1, \mu_{\theta i}) + w_{2,i}(J_{x,i}(u, 1, \theta_x) + J_{y,i}(u, 1, \theta_y))] \quad \text{s.t.: } \int_\Omega \mathrm{d}\Omega \le \mathrm{Vol}^* \tag{26}$$

where the weights are defined using Eqs. (25). The minimization of compliance problem with multiple loads cases can be solved by most existing methods [2,26]. Thus, the formulation for expected compliance obtained here is also valid for any computational topology optimization method that can solve the multiple load case problem. For the purpose of demonstration, this paper implements a level-set-based topology optimization, which is outlined in the following section.

The formulation, Eq. (26) can be implemented more efficiently by exploiting the linear elastic nature of the structure to reduce the number of load vectors needed when computing the displacement vectors for the required load cases [18]. In the general case $2n$ load vectors could be used to compute displacements for the $1 + 3n$ load cases.

The analytical formulation derived in this work only requires $1 + 3n$ load cases to accurately compute expected compliance and the required sensitivities. Therefore, the computational cost of computing the objective and sensitivities scales linearly with the number of loads with uncertainty. This is seen as more efficient than existing methods that rely on approximation or quadrate to define the required load cases. For example, if there are n loading uncertainties, including both magnitude and direction, and S is the number of samples or quadrate points used per uncertain variable, a total of S^n load cases could be required to compute the objective and sensitivities.

III. Level-Set-Based Topology Optimization

To solve Eq. (26) for continuum structures we use the level-set method with multiple load cases, where weights and load cases are defined to include the effects of uncertainties in loading through Eqs. (16), (20), (22), and (25). This section provides an overview of the level-set method for topology optimization and provides some details of our implementation [27]. First, the structure is defined as an implicit signed distance function $\phi(x)$, such that

$$\phi(x)\begin{cases} \ge 0 & x \in \Omega_s \\ =0 & x \in \Gamma \\ <0 & x \notin \Omega_s \end{cases} \tag{27}$$

where Ω_s is the domain of the structure and Γ is the structure boundary. A larger domain Ω, is defined to contain Ω_s and all possible solutions. Using the expressions developed in the previous section, the robust optimization problem of Eq. (2) under uncertainties in magnitude and direction of loading becomes a multiple load case problem:

$$\text{minimize}: E[J(u,f,\theta,\phi)] = \sum_{i=1}^{n} \int_{\Omega} J(u_i, f_i, \theta_i, \phi) H(\phi)\, \mathrm{d}\Omega$$
$$\text{s.t.:} \int_{\Omega} H(\phi)\, \mathrm{d}\Omega \leq \mathrm{Vol}^* \tag{28}$$

where $J(u_i, f_i, \theta_i, \phi)$ is the compliance computed for load case i, n is the number of required load cases and $H(x)$ is the Heaviside function. Assuming only surface traction loading, the shape derivative of objective $E[J(u,f,\theta,\phi)]$ is [26]

$$J'(u,\phi) = \sum_{i=1}^{n} \int_{\Gamma} J(u_i, f_i, \theta_i, \phi) V\, \mathrm{d}\Gamma \tag{29}$$

where V is a velocity function normal to the boundary.

Thus, V is chosen as $-\sum J(u_i, f_i, \theta_i, \phi)$, in order to reduce the objective towards its minimum [26]. However, the velocity function is modified to enforce the volume constraint by adding a constant λ to the velocity function. The constant is defined such that the volume constraint remains feasible, or approaches the feasible region. In our experience the relationship between λ and volume change is often found to be approximately linear. Hence λ can be efficiently calculated at each step using Newton's method and a numerical approximation to the boundary integral defining the volume change:

$$V = \lambda - \sum_{i=1}^{n} J(u_i, f_i, \theta_i, \phi) \tag{30}$$

A discretized Hamilton–Jacobi type equation for updating the level-set function $\phi(x)$ is defined as [3,4]

$$\phi_j^{k+1} = \phi_j^k - \Delta t V_j |\nabla \phi_j| \tag{31}$$

where j is a discrete grid point and Δt is the time step defined by the Courant–Friedrichs–Lewy condition for stability: $\Delta t = h/2|V_j|_{\max}$, h is the maximum grid spacing.

So far the velocity function defined in Eq. (30) is only applicable to the points along the structural boundary. To update the level-set function using Eq. (31), the discrete velocity values, V_j, have to be defined at all grid points. This is achieved using a velocity extension technique that extrapolates velocities away from the boundary [28]. To avoid evaluating the velocity function everywhere in the domain each iteration, the computation is limited to a narrow band around the boundary [29]. When the boundary approaches the edge of the narrow band then the band is redefined from the current boundary. However, this can lead to implicit functions that are too steep or shallow, which can reduce the accuracy and stability of the level-set method. Therefore, $\phi(x)$ is reinitialized to a signed distance function using the fast marching method [29] when the narrow band is redefined and also periodically to maintain accuracy and stability. The upwind finite difference scheme for gradient calculation is often employed by level-set methods due to its favorable stability [29]. This scheme is used here where each gradient component is approximated using the higher-order weighted essentially non-oscillatory method [30] which improves the stability and accuracy of the scheme.

The hole insertion method based on a pseudo third dimension [27] is employed to alleviate the well known problem of initial design dependent solutions in level-set methods [4]. The method is implemented with a narrow band width of $6h$, an initial pseudo thickness of h and a 2% upper limit on material removal due to hole creation during each iteration. For simplicity and efficiency when solving the finite element equation, level-set methods often employ a fixed regular mesh to discretize the design domain. However, some elements can be cut by the structure boundary leading to a discontinuity in material properties within the element. This problem is alleviated by employing the density approximation to the stiffness matrix of the cut elements [26]:

$$K_i = \frac{\alpha_i}{\alpha_t} K_t \tag{32}$$

where K_i is the approximated stiffness matrix for the cut element i, K_t is the stiffness matrix of a complete element, α_t is the complete element volume and α_i is the volume of structural material with element i. This approach is simple and efficient, but inaccuracies can occur when calculating boundary sensitivities defined by Eq. (29) [31]. Therefore, sensitivities are smoothed by a weighted least squares method using values calculated at Gauss points.

IV. Illustrative Examples

This section presents numerical examples using the level-set method, discussed in Sec. III, to solve the minimization of expected compliance problem of Eq. (26). This formulation accurately and efficiently computes the velocity function, Eq. (30). For all examples, Young's modulus and Poisson's ratio of 1.0 and 0.3 are used and design domains are discretized using unit sized square bilinear elements.

A. Simple Column

The simple two-dimensional structure shown in Fig. 1a is optimized for deterministic and uncertain loading conditions. The single point load f has mean magnitude $\mu = 10$ and mean applied direction $\mu_\theta = 3\pi/2$. To observe the effect of directional uncertainty on this simple example, the minimum expected compliance problem is solved for a range of applied direction standard deviations, $\sigma_\theta = 0.0, 0.1, 0.2, 0.3$, where $\sigma_\theta = 0.0$ is the deterministic case. The volume constraint for each problem was set to 20% of the design domain. For this example the inclusion of directional uncertainty only requires two load cases to accurately compute the expected compliance each iteration. The first load case is a unit load applied vertically with a weight of $50 \times [1 + \exp(-2\sigma_\theta^2)]$ and the second load case is a unit load applied horizontally with a weight of $50 \times [1 - \exp(-2\sigma_\theta^2)]$. These weights are calculated using Eqs. (25).

The deterministic solution is a straight column shown in Fig. 1b where all the material is aligned to support the vertically applied load. The expected compliance values for the deterministic solution under uncertain loading conditions are 1048.0, 2243.0, 4079.0 for $\sigma_\theta = 0.1$, 0.2, 0.3, respectively. This result demonstrates that expected compliance for a deterministic solution can increase as loading directional uncertainty increases. The solutions from the minimization of expected compliance problem, Fig. 2, produce arch type structures that are more robust against loading directional uncertainty. The values for expected compliance are 752.0 for $\sigma_\theta = 0.1$ (Fig. 2a), 900.0 for $\sigma_\theta = 0.2$ (Fig. 2b), and 1050.0 for $\sigma_\theta = 0.3$ (Fig. 2c), demonstrating improved performance over the deterministic solution. The volume of material present in the deterministic and robust solutions is the same and is on the prescribed limit. It also appears that the solutions from the robust optimization problem adapt to the level of uncertainty, as the width of the arch structure increases with increased variance. This simple example shows that more robust solutions can be obtained in the presence of loading direction uncertainty, as the expected compliance is significantly lower for the robust solutions compared with the deterministic one.

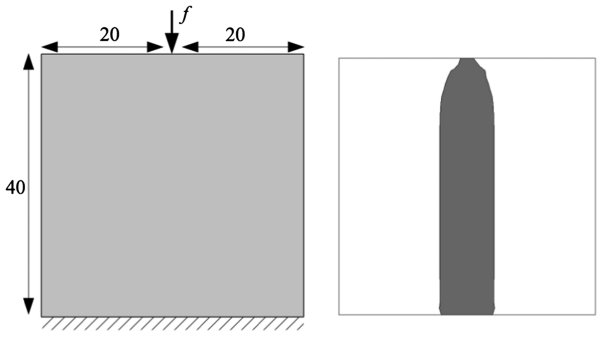

Fig. 1 Simple column example: a) geometry of initial design and b) deterministic solution, $\sigma_\theta = 0.0$.

a) b) c)

Fig. 2 Simple column robust solutions: a) $\sigma_\theta = 0.1$, b) $\sigma_\theta = 0.2$, and c) $\sigma_\theta = 0.3$.

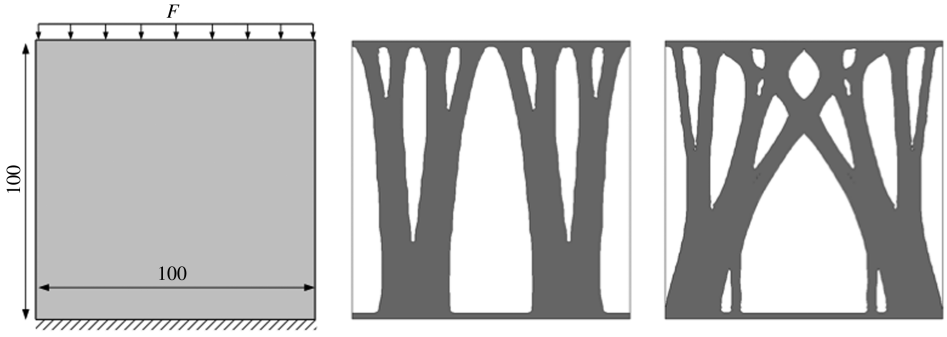

a) b) c)

Fig. 3 Carrier plate example: a) design domain and initial topology, b) deterministic solution ($\sigma_\theta = 0.0$), and c) robust solution ($\sigma_\theta = 0.25$).

B. Carrier Plate

A simple carrier plate example of Fig. 3a is used to demonstrate that the approach obtained in Sec. II for including uncertainty in loading can also be applied to distributed loads. The uniformly distributed load F has mean magnitude $\mu = 1.0$/unit length, mean applied direction $\mu_\theta = 3\pi/2$ and standard deviation $\sigma_\theta = 0.25$. To ensure the structure remains attached to the loading and boundary conditions during the optimization the bottom and top two rows of elements are fixed to remain part of the structure. The problem is solved for deterministic ($\sigma_\theta = 0.0$) and uncertain loading conditions. For this example the robust problem only requires two load cases. The first load case is a vertically applied uniformly distributed load with a magnitude of 1.0/unit length and a weight of 0.941. The second uniformly distributed load is applied in the horizontal direction along the top edge with a magnitude of 1.0/unit length and a weight of 0.059, where the weights are calculated using Eqs. (25). The volume constraint for both problems is set to 50% of the design domain.

The deterministic solution, Fig. 3b, contains members that are mainly aligned to withstand the uniformly distributed load. The deterministic compliance for this solution is 21.4×10^3, however, when the directional uncertainty is considered for the deterministic solution, the expected compliance increases significantly to 77.7×10^3. The robust solution depicted in Fig. 3c still contains some vertical members, but also possesses diagonal members able to cope with the uncertainty in the applied direction of the loading. The expected compliance for the robust solution is dramatically reduced to 33.6×10^3 demonstrating a significant increase in performance under uncertain loading direction compared with the deterministic solution. The convergence history of both solutions is depicted in Fig. 4.

C. Mast Structure

A mast structure, Fig. 5a, is designed for deterministic and uncertain loading conditions. The two vertical loads are considered

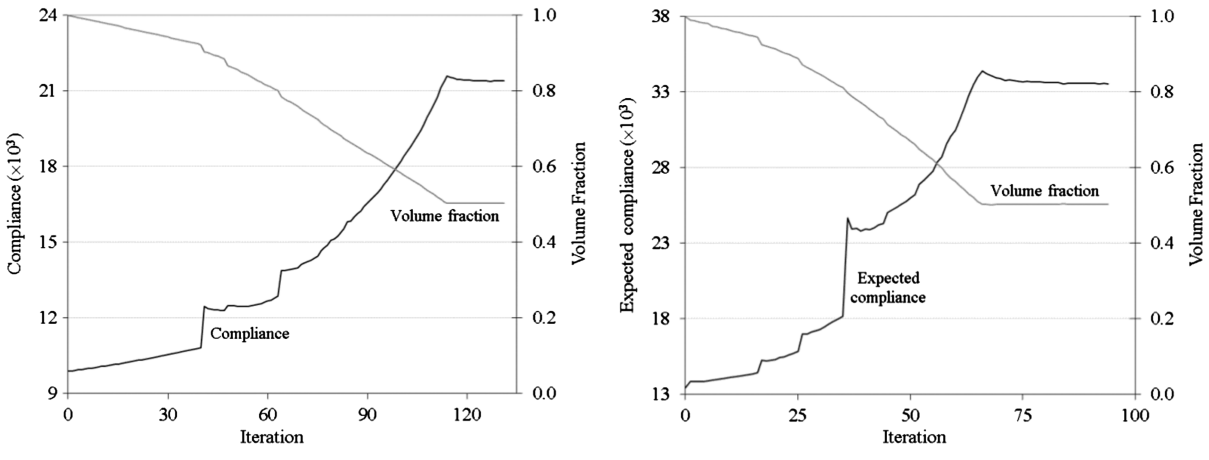

a) b)

Fig. 4 Carrier plate convergence history: a) deterministic solution and b) robust solution.

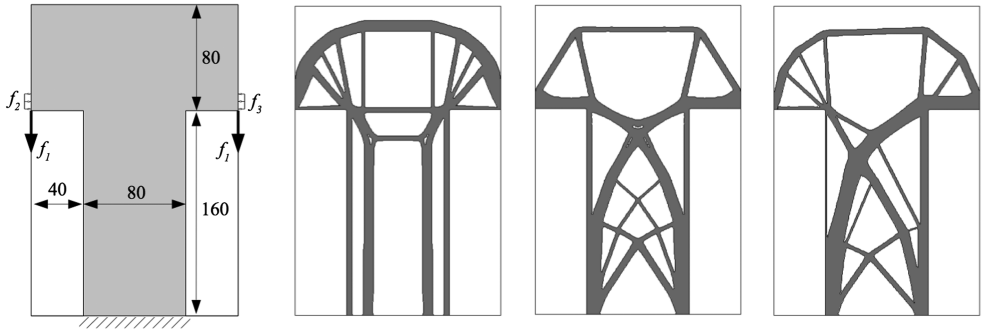

Fig. 5 Mast example: a) design domain and initial design, b) deterministic solution, c) robust solution ($\beta_2 = \beta_3 = 0.5$), and d) robust solution ($\beta_2 = 0.1$, $\beta_3 = 0.5$).

without uncertainty and both have a magnitude $f_1 = 5.0$. For this example the uncertainty exists in the magnitude of the horizontal side loads, where the uncertainty is modeled by a half-normal probability distribution:

$$P(x) = \sqrt{2/\pi\beta^2}\exp(-x^2/2\beta^2), \qquad x \in [0, \infty) \tag{33}$$

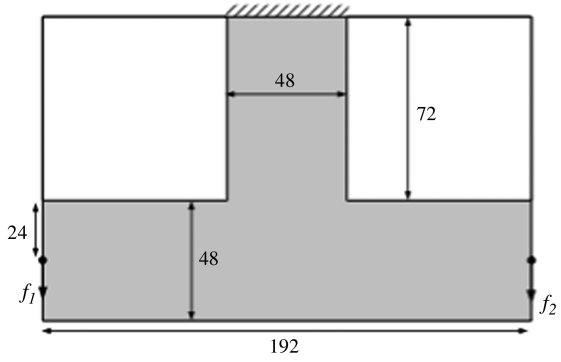

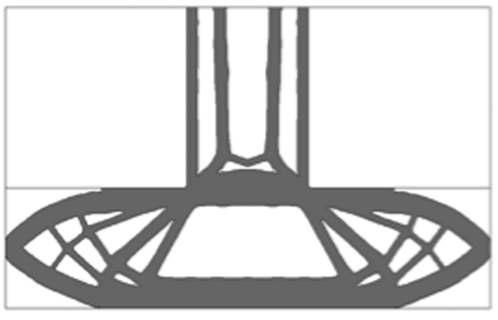

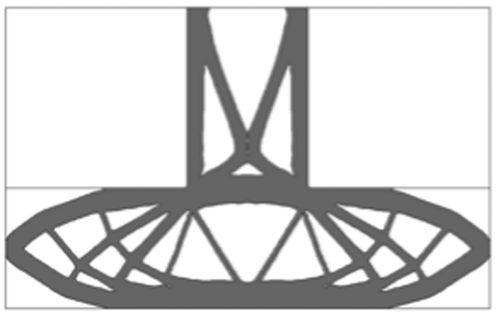

Fig. 6 Double hook example: a) design domain and initial topology, b) deterministic solution, and c) robust solution.

where β is the shape parameter of the distribution. Substituting Eq. (34) into Eq. (6) and evaluating between limits 0 to ∞ using the same integration by parts approach detailed in Sec. II.B yields the following equation for expected compliance:

$$E[J(u, f)] = \sum_{i=1}^{m} \kappa_{i,i}\beta_i^2 \tag{34}$$

Therefore, an additional load case of magnitude β_i is required for each magnitude uncertainty described by a half-normal distribution. This approach can be used to model uncertain loads that follow a Gaussian distribution, but are restricted to one sign, for example pressure loads such as wind and snow loading and reaction loads arising from tension cables. Two uncertain loading conditions are considered for the uniformly distributed side loads, f_2 and f_3. The first condition assumes both loads are described by identical probability distributions, $\beta_2 = \beta_3 = 0.5$. The second condition assumes the left side load has a lower mean, where $\beta_2 = 0.1$ and $\beta_3 = 0.5$. The volume constraint for each problem is set to 30% of the design domain.

The deterministic solution, without considering the side loads, Fig. 5b, contains vertical members in the central column aligned to carry the vertical loads. The deterministic compliance for this solution is 1.72×10^3, whereas the expected compliance considering the uncertain loads is 241.7×10^3 and 126.5×10^3 for the first and second uncertain conditions, respectively. The robust solution for the first uncertain loading condition, Fig. 5c, is achieved using just three load cases during each iteration. The solution is similar to the deterministic one, except that the central column has been reinforced with a cross braced structure and the structural components in the top section are reduced in size. This structural configuration helps to significantly lower the expected compliance, when compared with the deterministic solution, to 9.43×10^3. The second uncertain loading condition is now considered and the robust solution shown in Fig. 5d is obtained. This solution is similar to the first robust solution, however, there is an increased reinforcement to support the greater uncertain loading applied on the right hand side. This distribution of material produces an expected compliance of 5.75×10^3, which is again a significant improvement compared with the deterministic solution. This example demonstrates that a significant improvement in structural solutions with a marked difference in topology can be obtained when uncertain load cases are considered during optimization.

D. Combined Uncertainty Example

A double hook structure, Fig. 6a, is designed under deterministic and uncertain loading conditions where both loads have magnitude and directional uncertainties. For both loads f_1 and f_2, probability data are as follows: mean magnitude $\mu = 5.0$ and standard deviation $\sigma = 0.5$, mean loading direction $\mu_\theta = 3\pi/2$ and standard deviation $\sigma_\theta = 0.25$. Five load cases as defined by Eq. (26) are thus required to compute expected compliance with weights calculated using Eqs. (25). The first of these load cases is the simultaneous application

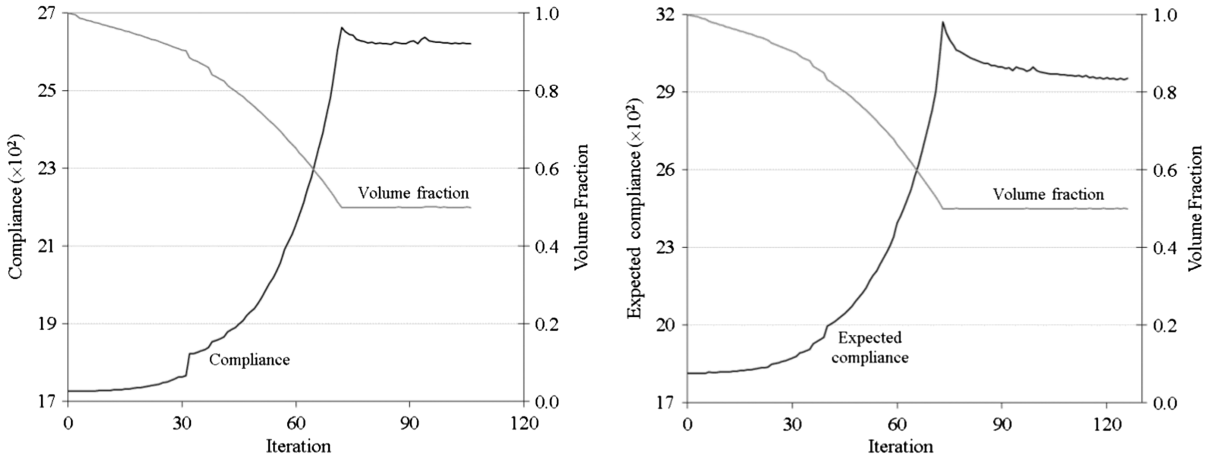

Fig. 7 Double hook convergence history: a) deterministic solution and b) robust solution.

of two vertical loads at the two loading points, where both loads have a magnitude of 4.846 and the load case weight is 1.0. The second case is a unit vertical load applied at loading point one with a weight of 1.483 and the third is a unit horizontal load with weight of 0.2797. The set of five load cases is completed by repeating the previous two load cases (with identical weights) for loading point two. The volume constraint for both problems is set to 50% of the design domain.

The deterministic problem produces a solution with deterministic compliance of 26.2×10^2, Fig. 6b. However, when uncertain loading conditions are applied to the deterministic solution, the expected compliance increases to 49.1×10^2. The robust solution is similar to the deterministic one except for the design of the central beam section, which is reinforced by cross braces, Fig. 6c. It is clear that this beam in the deterministic solution essentially acts like a tie-bar predominantly in tension, but the robust solution recognizes the bending due to the uncertain loading directions. The expected compliance of the robust solution is 29.4×10^2, again demonstrating an improved performance compared with the deterministic problem in the presence of uncertain loading conditions. Convergence histories for the two solutions are shown in Fig. 7.

It is interesting to note that if only magnitude uncertainties are considered, then expected compliance for the deterministic solution is 29.0×10^2. However, if only directional uncertainty is considered expected compliance is 46.3×10^2. This suggests that, for this example, the compliance of the deterministic solution is more sensitive to directional uncertainty compared with magnitude uncertainty.

V. Conclusions

This study posed a robust topology optimization problem as minimization of expected compliance. Loading uncertainty is considered in both direction and magnitude, where uncertain variables are described by normal probability distributions. Analytical expressions are derived to transform the expected compliance into a total compliance of a multiple load case problem. For a general problem only three additional cases per uncertain load are required to accurately compute compliance and sensitivities. Therefore, the approach is more efficient than the existing sampling or quadrature-based methods, especially for a large number of uncertainties.

The robust optimization problem is solved for continuum structures using the level-set method. The robust solutions show marked differences when compared with the equivalent deterministic cases. Furthermore, the expected compliance is significantly reduced compared with the deterministic solutions. This demonstrates the importance of including uncertainties in structural topology optimization methods to produce robust solutions.

We note that robustness can also be measured by the variability of the performance function and robust optimization can be posed as minimization of expected and variance of the performance. Including compliance variance in the presented formulation is the subject of our ongoing research.

Acknowledgments

The work reported in this paper has been undertaken as part of the Engineering and Physical Sciences Research Council funded Innovative Design and Manufacturing Research Center at the University of Bath and this support is gratefully acknowledged. The authors would also like to thank the Numerical Analysis Group at the Rutherford Appleton Laboratory for their FORTRAN Harwell Subroutine Library packages.

References

[1] Choi, S.-K., Grandhi, R. V., and Canfield, R. A., *Reliability-Based Structural Design*, Springer, London, 2007, pp. 1–306.

[2] Bendsøe, M. P., and Sigmund, O., *Topology Optimization: Theory, Methods and Applications*, Springer–Verlag, Germany, 2004, pp. 1–370.

[3] Wang, M. Y., Wang, X., and Guo, D., "A Level Set Method for Structural Topology Optimization," *Computer Methods in Applied Mechanics and Engineering*, Vol. 192, Nos. 1–2, 2003, pp. 227–246. doi:10.1016/S0045-7825(02)00559-5

[4] Allaire, G., Jouve, F., and Toader, A., "Structural Optimization Using Sensitivity Analysis and a Level-Set Method," *Journal of Computational Physics*, Vol. 194, No. 1, 2004, pp. 363–393. doi:10.1016/j.jcp.2003.09.032

[5] Krog, L., Tucker, A., Kemp, M., and Boyd, R., "Topology Optimization of Aircraft Wing Box Ribs," 10th AIAA/ISSMO Multidisciplinary Analysis and Optimization Conference, Albany, NY, AIAA Paper 2004-4481, 2004.

[6] Gomes, A. A., and Suleman, A., "Topology Optimization of a Reinforced Wing Box for Enhanced Roll Maneuvers," *AIAA Journal*, Vol. 46, No. 3, 2008, pp. 548–556. doi:10.2514/1.23028

[7] Kharmanda, G., Olhoff, N., Mohamed, A., and Lemaire, M., "Reliability-Based Topology Optimization," *Structural and Multidisciplinary Optimization*, Vol. 26, No. 5, 2004, pp. 295–307. doi:10.1007/s00158-003-0322-7

[8] Jung, H. S., and Cho, S., "Reliability-Based Topology Optimization of Geometrically Nonlinear Structures with Loading and Material Uncertainties," *Finite Elements in Analysis and Design*, Vol. 41, No. 3, 2004, pp. 311–331. doi:10.1016/j.finel.2004.06.002

[9] Kim, C., Wang, S. Y., Bae, K. R., Moon, H., and Choi, K. K., "Reliability-Based Topology Optimization with Uncertainties," *Journal of Mechanical Science and Technology*, Vol. 20, No. 4, 2006, pp. 494–504.

[10] Mogami, K., Nishiwaki, S., Izui, K., Yoshimura, M., and Kogiso, N., "Reliability-Based Structural Optimization of Frame Structures for Multiple Failure Criteria Using Topology Optimization Techniques," *Structural and Multidisciplinary Optimization*, Vol. 32, No. 4, 2006, pp. 299–311.

doi:10.1007/s00158-006-0039-5
[11] Logo, J., "New Type of Optimality Criteria Method in Case of Probabilistic Loading Conditions," *Mechanics Based Design of Structures and Machines*, Vol. 35, No. 2, 2007, pp. 147–162. doi:10.1080/15397730701243066
[12] Luo, Y., Kang, Z., Luo, Z., and Li, A., "Continuum Topology Optimization with Nonprobabilistic Reliability Constraints Based on Multi-Ellipsoid Convex Model," *Structural and Multidisciplinary Optimization*, Vol. 39, No. 3, 2009, pp. 297–310. doi:10.1007/s00158-008-0329-1
[13] Kang, Z., and Luo, Y., "Reliability-Based Structural Optimization with Probability and Convex Set Hybrid Models," *Structural and Multidisciplinary Optimization*, Vol. 42, No. 1, 2009, pp. 89–102. doi:10.1007/s00158-009-0461-6
[14] Silva, M., Tortorelli, D. A., Norato, J. A., Ha, C., and Bae, H-R., "Component and System Reliability-Based Topology Optimization Using a Single-Loop Method," *Structural and Multidisciplinary Optimization*, Vol. 41, No. 1, 2010, pp. 87–106. doi:10.1007/s00158-009-0401-5
[15] Calafiore, G. C., and Dabbene, F., "Optimization Under Uncertainty with Applications to Design of Truss Structures," *Structural and Multidisciplinary Optimization*, Vol. 35, No. 3, 2008, pp. 189–200. doi:10.1007/s00158-007-0145-z
[16] de Gournay, F., Allaire, G., and Jouve, F., "Shape and Topology Optimization of the Robust Compliance via the Level Set Method," *ESAIM: Control, Optimisation and Calculus of Variations*, Vol. 14, No. 1, 2008, pp. 43–70. doi:10.1051/cocv:2007048
[17] Kang, Z., and Luo, Y., "Non-Probabilistic Reliability-Based Topology Optimization of Geometrically Nonlinear Structures Using Convex Models," *Computer Methods in Applied Mechanics and Engineering*, Vol. 198, Nos. 41–44, 2009, pp. 3228–3238. doi:10.1016/j.cma.2009.06.001
[18] Conti, S., Held, H., Pach, M., Rumpf, M., and Schultz, R., "Shape Optimization Under Uncertainty: A Stochastic Programming Perspective," *SIAM Journal on Optimization*, Vol. 19, No. 4, 2009, pp. 1610–1632. doi:10.1137/070702059
[19] Evgrafov, A., and Patriksson, M., "Stochastic Structural Topology Optimization: Discretization and Penalty Function Approach," *Structural and Multidisciplinary Optimization*, Vol. 25, No. 3, 2003, pp. 174–188. doi:10.1007/s00158-003-0290-y
[20] Chen, S., Chen, W., and Lee, S., "Level Set Based Robust Shape and Topology Optimization Under Random Field Uncertainties," *Structural and Multidisciplinary Optimization*, Vol. 41, No. 4, 2010, pp. 507–524. doi:10.1007/s00158-009-0449-2
[21] Doltsinis, I., and Kang, Z., "Robust Design of Structures Using Optimization Methods," *Computer Methods in Applied Mechanics and Engineering*, Vol. 193, Nos. 23–26, 2004, pp. 2221–2237. doi:10.1016/j.cma.2003.12.055
[22] Kogiso, N., Ahn, W., Nishiwaki, S., Izui, K., and Yoshimura, M., "Robust Topology Optimization for Compliant Mechanisms Considering Uncertainty of Applied Loads," *Journal of Advanced Mechanical Design Systems and Manufacturing*, Vol. 2, No. 1, 2008, pp. 96–107. doi:10.1299/jamdsm.2.96
[23] Schueller, G., and Jensen, H., "Computational Methods in Optimization Considering Uncertainties: An Overview," *Computer Methods in Applied Mechanics and Engineering*, Vol. 198, No. 1, 2008, pp. 2–13. doi:10.1016/j.cma.2008.05.004
[24] Alvarez, F., and Carrasco, M., "Minimization of the Expected Compliance as an Alternative Approach to Multiload Truss Optimization," *Structural and Multidisciplinary Optimization*, Vol. 29, No. 6, 2005, pp. 470–476. doi:10.1007/s00158-004-0488-7
[25] Guest, J., and Igusa, T., "Structural Optimization Under Uncertain Loads and Nodal Locations," *Computer Methods in Applied Mechanics and Engineering*, Vol. 198, No. 1, 2008, pp. 116–124. doi:10.1016/j.cma.2008.04.009
[26] Allaire, G., and Jouve, F., "A Level-Set Method for Vibration and Multiple Loads Structural Optimization," *Computer Methods in Applied Mechanics and Engineering*, Vol. 194, Nos. 30–33, 2005, pp. 3269–3290. doi:10.1016/j.cma.2004.12.018
[27] Dunning, P., and Kim, H. A., "A New Hole Insertion Method for Level Set Based Topology Optimization," 13th AIAA/ISSMO Multidisciplinary Analysis Optimization Conference, Fort Worth, TX, AIAA Paper 2010-9316, 13–15 Sept. 2010.
[28] Adalsteinsson, D., and Sethian, J., "The Fast Construction of Extension Velocities in Level Set Methods," *Journal of Computational Physics*, Vol. 148, No. 1, 1999, pp. 2–22. doi:10.1006/jcph.1998.6090
[29] Sethian, J. A., *Level Set Methods and Fast Marching Methods*, 2nd ed., Cambridge Univ. Press, New York, 1999, pp. 47, 80–90.
[30] Mei, Y. L., and Wang, X., "A Level Set Method for Structural Topology Optimization and its Applications," *Advances in Engineering Software*, Vol. 35, No. 7, 2004, pp. 415–441. doi:10.1016/j.advengsoft.2004.06.004
[31] Dunning, P., Kim, H. A., and Mullinuex, G., "Error Analysis of Fixed Grid Formulation for Boundary Based Structural Optimization," *Proceedings of the 7th ASMO UK Conference on Engineering Design Optimization*, ASMO-UK, Univ. of Leeds, U.K., 2008, pp. 137–146.

A. Messac
Associate Editor